Weighted Sum-Rate Maximization for Distributed RIS-Assisted Cell-Free Massive MIMO

Diluka Loku Galappaththige[1], Dhanushka Kudathanthirige[2], Gayan Amarasuriya[3], and Chintha Tellambura[1]
[1]Department of Electrical and Computer Engineering, University of Alberta, Edmonton, AB, T6G 1H9, Canada
[2]Department of Physics and Engineering, Cornell College, Mount Vernon, IA, 52314, USA
[3]School of Electrical, Computer, and Biomedical Engineering, Southern Illinois University, Carbondale, IL, 62901, USA
Email: diluka.lg@ualberta.ca, dkudathanthirige@cornellcollege.edu, gayan.baduge@siu.edu, ct4@ualberta.ca

***Abstract*—The feasibility of utilizing distributed reconfigurable intelligent surfaces (RISs) in a cell-free massive multiple-input multiple-output (mMIMO) setup is investigated in this study. To maximize the system-wide achievable weighted sum-rate under a transmit power constraint at the access points (APs), a joint optimization problem is formulated for optimizing the transmit/active beamformers at the APs and reflective/passive beamforming at the distributed RISs. The proposed joint optimization problem is solved by using a fractional programming-based alternate optimization method. A comprehensive set of numerical results is presented to evaluate the performance of the proposed system model and optimization framework. Moreover, the convergence and computational complexity aspects of the proposed algorithm, and the effects of the numbers of APs, RISs, and reflecting elements are investigated through our analytical and simulation results. Consequently, we reveal that the proposed distributed RIS-assisted cell-free mMIMO system model helps next-generation wireless architectures to obtain high spectral efficiency gains.**

I. Introduction

Massive multiple-input multiple-output (mMIMO), which aggressively uses spatial multiplexing gains available to large antenna arrays, has been identified as a critical technology for the fifth-generation (5G) and beyond. However, when network density increases, inter-cell interference becomes a significant bottleneck in conventional cell-based mMIMO systems [1]. Consequently, cell-free mMIMO systems can offer a higher coverage probability than the conventional co-located mMIMO systems at the expense of additional front-haul/back-haul requirements [2], [3]. Thus, a cell-free mMIMO architecture, a variation of distributed mMIMO architecture, has recently caught the interest of the wireless research community because of its potential to utilize macro-diversity gains against large-scale fading effects [2], [3].

Because of its inherent advantages, cell-free mMIMO is a vital candidate technology for the next-generation of wireless systems [2], [3]. Specifically, cell-free systems can provide enhanced spatial and energy efficiency gains by eliminating impediments rendered by spatial-correlated fading in co-located antenna arrays and minimizing shadow fading effects [2], [3]. Cell-free mMIMO systems can loosen cell boundaries and hence allow numerous access points (APs) to be geographically distributed to provide a uniformly better quality-of-service (QoS) to all users over a much larger geographical area [2], [3]. In a cell-free setup, the front-haul/back-haul link connects all the APs to a central processing unit (CPU), and the APs simultaneously serve all the users in an area.

On a parallel avenue, a revolutionary concept of covering physical objects within a wireless propagation environment with reconfigurable intelligent surfaces (RISs) has recently emerged, attracting the interest of both academia and industry [4], [5]. A RIS is made up of numerous passive reflectors with adjustable reflecting coefficients that enable impinging electromagnetic signals to propagate with the desired characteristics [4], [5]. These adjustable phase shifts can enable constructive or destructive signal combinations at the desired destination, improving the signal-to-noise ratio (SNR) and minimizing the co-channel interference [6]. This results in the recycling of electromagnetic (EM) waves within a propagation medium, leading to high spectrum and energy efficiency gains. For nearly a century, classical communication theory has presumed that the channel between the transmitter and receiver is not open for optimization. Instead, it is customary to optimize many parameters such as precoding, beamforming, power allocation, and others. But such approaches have now reached the law of diminishing returns. Hence, RISs move this paradigm such that the channel itself becomes an additional variable that can be optimized on the fly [4], [5].

A. Prior Related Research

References [2], [3] study the fundamental notion of the cell-free architecture and compare the performance of such systems to conventional co-located systems. These findings show that the former can outperform the co-located mMIMO by offering uniformly better QoS to the users, minimizing spatial correlation, and reducing effective transmission distances to improve overall energy and spectral efficiency. The fundamental RIS design concepts are presented in [4], [5]. By utilizing ray-tracing techniques, [7] proposes a new path-loss/propagation framework for modeling RIS-assisted wireless channels. The authors of [8] utilize semi-definite relaxation and alternative optimization approaches to investigate the joint optimization of the base-station precoder and RIS phase-shifts. Reference [6] investigates the fundamental performance limits of distributed RIS-assisted end-to-end channels with the Nakagami-m fading model.

The authors of [9] investigate the feasibility of employing RISs within a cell-free setup. They derive the fundamental performance metrics for the single-user case by statistically characterizing the optimal SNR at the user. Reference [10] studies a multiple RIS-assisted cell-free mMIMO system without direct channels between the APs and users. Reference [10] proposes alternative optimization approaches for optimizing active and passive beamforming at the APs and RISs to maximize the sum-rate. Using the incremental alternating direction method of multipliers, [11] develops a decentralized optimization framework for AP's digital beamformers and RIS's passive beamformers in a cell-free system. Reference [12] analyses the uplink performance of a RIS-assisted cell-free mMIMO system by utilizing the zero-forcing receiver. This work derives a closed-form expression for the system's achievable rate. The authors of [13] derive the closed-form achievable rate for a RIS-assisted cell-free mMIMO under imperfect channel state information (CSI) and thereby demonstrate that the system's performance is independent of the RIS phase configuration under Rayleigh fading and the direct channel estimation protocol. Reference [14] presents a hybrid-beamforming scheme to maximize the energy efficiency of a RIS-assisted cell-free MIMO system by proposing an iterative-based energy efficiency maximization algorithm.

B. Motivation and Our Contribution

The purpose of this paper is to investigate RISs to improve the performance of cell-free mMIMO systems. We naturally anticipate synergistic benefits of cell-free architectures and RIS-assisted communication. Specifically, we would expect an increase of the sum-rate if the beamforming options are properly optimized. Hence, we formulate a weighted sum-rate maximization problem considering transmit beamforming at the APs and reflective beamforming at the RISs for a generalized RIS-assisted cell-free mMIMO system model as shown in Fig. 1. Thereby, we aim to address the following gaps in the literature:

1) *Lack of a generalized system model:* Prior integrated RIS and cell-free mMIMO models are lacking some details. In contrast, Fig. 1 captures the most generic system setup that is practically viable, where users may or may not experience direct and reflection channels. Although [10] investigates a special case the RIS-assisted cell-free mMIMO setup, to reduce the complexity of the optimization problem, [10] omits the presence of direct channels between the APs and users.
2) *Lack of weighted sum-rate maximization:* Since the users in the network may have different QoS requirements, and thus the weighted sum-rate maximization will ensure that we meet those requirements. Despite noteworthy prior research [9]–[14], to the best of our knowledge, no study has focused on a weighted sum-rate maximization framework for the generalized RIS-assisted cell-free mMIMO and its performance evaluation.

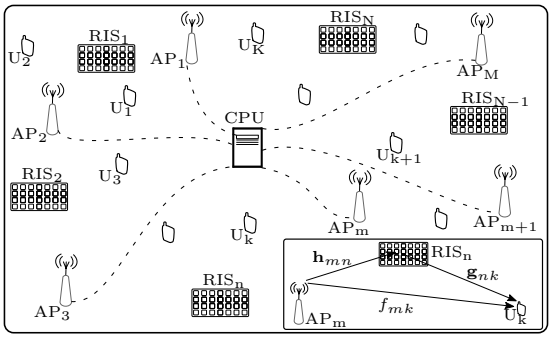

Fig. 1. System model - A distributed RIS-assisted communication setup.

In this paper, we consider a practically feasible generalized RIS-assisted cell-free mMIMO system by motivating these facts. Therefore, we develop a novel optimization framework for maximizing its sum-rate. We utilize the alternating optimization framework, and our sum-rate metric is system-wide weighted to accommodate the various QoS requirements of different users. We thus jointly optimize the transmit beamformers at the APs and phase-shifters at the distributed RISs.

Due to the intricately coupled variables in the signal-to-interference-plus-noise ratio (SINR), this problem is non-convex with non-convex objective and constraint, and difficult to solve optimally in general. Hence, we decouple it into two sub-problems $\mathcal{P}_w$ and $\mathcal{P}_\theta$. We reformulate $\mathcal{P}_w$ and $\mathcal{P}_\theta$ to become convex and solve iteratively using a fractional programming-based alternative optimization technique [15], [16]. We also present numerical results to investigate the performance of the proposed system and the optimization framework.

Our simulation results reveal that the proposed techniques outperform the conventional cell-free mMIMO and the RIS-assisted case with random beamforming in the achievable sum-rate. Moreover, we investigate the impact of the numbers of APs, RISs, and reflecting elements at the distributed RISs. Consequently, our numerical results advocate that next-generation wireless systems deploy RIS-assisted cell-free systems to boost spectral efficiency.

Notation: An uppercase boldface letter represents a matrix, a lowercase boldface letter represents a vector, and a non-bold italic letter denotes a scalar. The notations, $\mathbf{x}^T$, $\mathbf{x}^*$, and $\mathbf{x}^H$ denote the transpose, conjugate, and conjugate-transpose of $\mathbf{x}$, respectively. $\mathbb{E}[X]$ and $\mathbb{V}\mathrm{ar}[X]$ represent the expectation and variance of a random variable X, respectively. $X \sim \mathcal{N}\left(\mu_X, \sigma_X^2\right)$ denotes that X is Gaussian distributed with μ_X mean and σ_X^2 variance. The notation, $\mathrm{bdiag}\left(\cdot\right)$, denotes the block diagonal operator.

II. System, Channel, and Signal Models

A. System and Channel Models

We consider a distributed RIS-assisted cell-free mMIMO system in which M number of single-antenna APs simultaneously serve K single-antenna users through N distributed RISs, each having L passive reflective elements as shown in Fig. 1. It is assumed that the phase-shifts of the incident EM waves at the

RIS reflecting elements can be intelligently controlled to have constructive or destructive addition at a desired location [8]. For the sake of notation brevity, we denote the set of APs as $\mathcal{M} = \{1, \cdots, M\}$, the set of RISs as $\mathcal{N} = \{1, \cdots, N\}$, and the set of users as $\mathcal{K} = \{1, \cdots, K\}$.

The direct channel between the mth AP and the kth user is denoted by f_{mk}, while $\mathbf{h}_{mn} \in \mathbb{C}^{L\times 1}$ and $\mathbf{g}_{nk}^H \in \mathbb{C}^{1\times L}$ represent the channels between the mth AP and the nth RIS, and the nth RIS and the kth user, respectively. The aforementioned channels are modeled as

$$\mathbf{v}_{ab} = \zeta_{v_{ab}}^{1/2} \tilde{\mathbf{v}}_{ab}, \tag{1}$$

where $\mathbf{v} \in \{f, \mathbf{h}, \mathbf{g}\}$, $a \in \{m, , n\}$, and $b \in \{n, k\}$. Here, $\tilde{\mathbf{v}}_{ab} \sim \mathcal{CN}_{1\times Q}\left(\mathbf{0}_{1\times Q}, \mathbf{I}_{Q\times Q}\right)$ captures the quasi-static Rayleigh fading, where $Q \in \{1, L\}$, and $\zeta_{v_{ab}}$ accounts for path-loss/shadowing, which is typically assumed to be fixed for many coherence intervals [3]. Thus, these long-term channel statistics are assumed to be know a-prior because they change very slowly, and it is sufficient to estimate them once every tens/hundreds of coherence intervals [3].

B. Signal Model

The signal transmitted by the mth AP is given as

$$x_m = \sqrt{P} \sum\nolimits_{k\in\mathcal{K}} w_{mk} q_k, \tag{2}$$

where P is the transmit power at the mth AP, $w_{mk} \in \mathbb{C}^{1\times 1}$ is the linear precoder at the mth AP for the kth user, and q_k denotes the signal intended for the kth user satisfying $\mathbb{E}\left[|q_k|^2\right] = 1$. Then, the signal received at the kth user can be written as

$$r_k = \sum\nolimits_{m\in\mathcal{M}} \left(f_{mk} + \sum\nolimits_{n\in\mathcal{N}} \mathbf{g}_{nk}^H \mathbf{\Theta}_n \mathbf{h}_{mn}\right) x_m + n_k, \tag{3}$$

where x_m is the transmitted signal by the mth AP (2), and n_k is an additive white Gaussian noise (AWGN) at the kth user having zero mean and variance of σ_N^2 such that $n_k \sim \mathcal{CN}(0, \sigma_N^2)$. In (3), $\mathbf{\Theta}_n = \operatorname{diag}\left(\theta_{n1}, \cdots, \theta_{nl}, \cdots, \theta_{nL}\right) \in \mathbb{C}^{L\times L}$ is a diagonal matrix, which captures the reflection properties of the nth RIS. Moreover, θ_{nl} is a complex-valued reflection coefficient at the lth reflective element of the nth RIS. First, defining $\mathbf{f}_k^H = [f_{1k}, \cdots, f_{mk}, \cdots, f_{Mk}] \in \mathbb{C}^{1\times M}$, $\mathbf{H}_n = [\mathbf{h}_{1n}, \cdots, \mathbf{h}_{mn}, \cdots, \mathbf{h}_{Mn}] \in \mathbb{C}^{L\times M}$, and $\mathbf{w}_i^H = [w_{1i}, \cdots, w_{mi}, \cdots, w_{Mi}] \in \mathbb{C}^{1\times M}$, then substituting (2) into (3), the received signal at the kth user (3) can be rearranged as follows:

$$r_k = \sqrt{P} \underbrace{\left(\mathbf{f}_k^H + \sum\nolimits_{n\in\mathcal{N}} \mathbf{g}_{nk}^H \mathbf{\Theta}_n \mathbf{H}_n\right) \mathbf{w}_k q_k}_{\text{Desired signal}} + \sqrt{P} \underbrace{\sum\nolimits_{i\in\mathcal{K}'} \left(\mathbf{f}_k^H + \sum\nolimits_{n\in\mathcal{N}} \mathbf{g}_{nk}^H \mathbf{\Theta}_n \mathbf{H}_n\right) \mathbf{w}_i q_i}_{\text{Inter-user Interference}} + n_k, \tag{4}$$

where $\mathcal{K}' = \mathcal{K}/\{k\}$. Then, the received SINR at the kth user is derived via (4) as

$$\gamma_k = \frac{P\left|\left(\mathbf{f}_k^H + \sum_{n\in\mathcal{N}} \mathbf{g}_{nk}^H \mathbf{\Theta}_n \mathbf{H}_n\right) \mathbf{w}_k\right|^2}{P\sum_{i\in\mathcal{K}'}\left|\left(\mathbf{f}_k^H + \sum_{n\in\mathcal{N}} \mathbf{g}_{nk}^H \mathbf{\Theta}_n \mathbf{H}_n\right) \mathbf{w}_i\right|^2 + \sigma_N^2}. \tag{5}$$

Next, the achievable rate at the kth user and the system-wide sum-rate are defined as

$$\mathcal{R}_k = \log_2\left(1 + \gamma_k\right), \tag{6}$$

$$\mathcal{R} = \sum\nolimits_{i\in\mathcal{K}} \mathcal{R}_i = \sum\nolimits_{i\in\mathcal{K}} \log_2\left(1 + \gamma_i\right), \tag{7}$$

where γ_k is defined in (5).

III. Problem Formulation

In this section, we jointly optimize the transmit beamformers at the APs and phase-shift matrices at the distributed RISs to maximize the system-wide achievable weighted sum-rate. To this end, the proposed joint optimization problem can be formulated as follows:

$$\mathcal{P}_1 : \underset{\mathbf{W}, \mathbf{\Theta}_n \forall n}{\text{maximize}} \sum\nolimits_{i\in\mathcal{K}} \alpha_i \log_2\left(1 + \gamma_i\right), \tag{8a}$$

$$\text{subject to} \sum\nolimits_{i\in\mathcal{K}} |w_{mi}|^2 \le 1, \forall m, \tag{8b}$$

$$|\theta_{nl}| \le 1, \forall n, l, \tag{8c}$$

where $\mathbf{W} = [\mathbf{w}_1, \cdots, \mathbf{w}_k, \cdots, \mathbf{w}_K] \in \mathbb{C}^{M\times K}$, and γ_i is defined in (5). Moreover, α_i denotes the priority assigned for the ith user such that $0 \le \alpha_i \le 1$ and $\sum_{i\in\mathcal{K}} \alpha_i = 1$. Here, a larger α_i value refers to a higher priority. Due to the non-convex objective function (8a), the problem $\mathcal{P}_1$ cannot be solved via conventional convex optimization methods. Hence, in this paper, we aim to find a sub-optimal solution for $\mathcal{P}_1$ by decoupling the optimization variables, $\mathbf{W}$ and $\mathbf{\Theta}_n$, to reduce $\mathcal{P}_1$ into two sub-problems. Thus, for given $\mathbf{\Theta}_n, \forall n$, $\mathcal{P}_1$ can be reduced to a transmit beamforming optimization problem and can be formulated as

$$\mathcal{P}_w : \underset{\mathbf{W}}{\text{maximize}} \sum\nolimits_{i\in\mathcal{K}} \alpha_i \log_2\left(1 + \gamma_i\right), \tag{9a}$$

$$\text{subject to} \sum\nolimits_{i\in\mathcal{K}} |w_{mi}|^2 \le 1, \forall m. \tag{9b}$$

Similarly, for given $\mathbf{W}$, $\mathcal{P}_1$ becomes a phase-shift optimization problem for the distributed RISs. Thus, the corresponding optimization problem for $\mathbf{\Theta}_n, \forall n$ can be formulated as

$$\mathcal{P}_\theta : \underset{\mathbf{\Theta}}{\text{maximize}} \sum\nolimits_{i\in\mathcal{K}} \alpha_i \log_2\left(1 + \gamma_i\right), \tag{10a}$$

$$\text{subject to } |\theta_{nl}| \le 1, \forall n, l, \tag{10b}$$

where $\mathbf{\Theta} = \operatorname{bdiag}\left(\mathbf{\Theta}_1, \cdots, \mathbf{\Theta}_N\right)$. It is worth noting that $\mathcal{P}_w$ and $\mathcal{P}_\theta$ are still not convex since the corresponding objective functions are not convex function in either of the optimization variables. Now, we adopt an alternating optimization technique in which $\mathcal{P}_w$ and $\mathcal{P}_\theta$ are maximized in an alternating manner until the weighted sum-rate objective converges. In the following subsections, we develop the proposed optimization algorithms for solving $\mathcal{P}_w$, $\mathcal{P}_\theta$, and overall problem $\mathcal{P}_1$.

A. Transmit Beamforming

First, we define the superimposed/composite channel for the kth user as $\mathbf{u}_k^H \triangleq \left(\mathbf{f}_k^H + \sum_{n\in\mathcal{N}} \mathbf{g}_{nk}^H \mathbf{\Theta}_n \mathbf{H}_n\right)$, and then the SINR in (5) can be rewritten as

$$\gamma_k = \frac{P\left|\mathbf{u}_k^H \mathbf{w}_k\right|^2}{P\sum_{i\in\mathcal{K}'}\left|\mathbf{u}_k^H \mathbf{w}_i\right|^2 + \sigma_N^2}. \tag{11}$$

By introducing a new variable (β_i) to replace the SINR terms in the objective function (9a) such that $\beta_i \leq \gamma_i$, $\mathcal{P}_w$ can be reformulated as

$$\mathcal{P}_{w_1}: \underset{\mathbf{W},\boldsymbol{\beta}}{\text{maximize}} \sum\nolimits_{i\in\mathcal{K}} \alpha_i \log_2\left(1+\beta_i\right), \tag{12a}$$

$$\text{subject to} \sum\nolimits_{i\in\mathcal{K}} |w_{mi}|^2 \leq 1, \forall m, \tag{12b}$$

$$\beta_k \leq \frac{P\left|\mathbf{u}_k^H\mathbf{w}_k\right|^2}{P\sum_{i\in\mathcal{K}'}\left|\mathbf{u}_k^H\mathbf{w}_i\right|^2+\sigma_N^2}, \forall k, \tag{12c}$$

where $\boldsymbol{\beta} = [\beta_1, \cdots, \beta_K]^T$. The above optimization can be separated into two parts: an outer optimization over $\mathbf{W}$ and an inner optimization over $\boldsymbol{\beta}$ with fixed $\mathbf{W}$. The inner optimization is a convex optimization in $\boldsymbol{\beta}$, and hence, the strong duality holds [15]. The obvious solution to this inner optimization is for β_k to satisfy (12c) with equality. We use the Lagrangian dual transform to handle the logarithm in the objective function of $\mathcal{P}_{w_1}$ [15], and the corresponding Lagrangian function can be written as

$$L(\boldsymbol{\beta},\mathbf{y}) = \sum\nolimits_{k\in\mathcal{K}} \alpha_k \log_2\left(1+\beta_k\right) - \sum\nolimits_{k\in\mathcal{K}} y_k\left(\beta_k - \frac{P\left|\mathbf{u}_k^H\mathbf{w}_k\right|^2}{P\sum_{i\in\mathcal{K}'}\left|\mathbf{u}_k^H\mathbf{w}_i\right|^2+\sigma_N^2}\right), \tag{13}$$

where $\mathbf{y} = [y_1, \cdots, y_K]^T$ is the dual variable vector introduced for each inequality constraint in (12c). From the strong duality, $\mathcal{P}_{w_1}$ can be equivalently reformulated to a dual problem as

$$\mathcal{P}_{w_2}: \underset{\mathbf{y}\succeq 0}{\text{minimize}} \quad \underset{\boldsymbol{\beta}}{\text{maximize}} \quad L(\boldsymbol{\beta},\mathbf{y}). \tag{14}$$

From the first-order condition $\partial L(\boldsymbol{\beta},\mathbf{y})/\partial\beta_k$, the optimal solution of y_k can be obtained as

$$y_k^o = \frac{\alpha_k\left(P\sum_{i\in\mathcal{K}'}\left|\mathbf{u}_k^H\mathbf{w}_i\right|^2+\sigma_N^2\right)}{\ln(2)\left(P\sum_{i\in\mathcal{K}}\left|\mathbf{u}_k^H\mathbf{w}_i\right|^2+\sigma_N^2\right)}. \tag{15}$$

It is worth noting that $y_k \geq 0$ is automatically satisfied for this particular case. Thus, by using (15) and (14), the inner optimization can be reformulated as

$$\mathcal{P}_{w_3}: \underset{\boldsymbol{\beta}}{\text{maximize}} \quad L(\boldsymbol{\beta},\mathbf{y}^o). \tag{16}$$

Furthermore, when combined with the outer maximizing over $\mathbf{W}$ and after several mathematical formulations, it can be shown that the solution to $\mathcal{P}_{w_3}$ also satisfies $\mathcal{P}_{w_1}$. The proposed algorithm for the above formulation is given in Algorithm 1, and the detailed derivations are omitted due to the page limitation [15], [16].

B. Phase-Shift Optimization

We define $\mathbf{g}_k^H = [\mathbf{g}_{1k}^H, \cdots, \mathbf{g}_{Nk}^H]$ and $\mathbf{H} = [\mathbf{H}_1; \cdots; \mathbf{H}_N]$. Thereby, the SINR in (5) is rearranged as follows:

$$\gamma_k = \frac{P\left|b_{kk}+\boldsymbol{\theta}^H\mathbf{a}_{kk}\right|^2}{P\sum_{i\in\mathcal{K}'}\left|b_{ik}+\boldsymbol{\theta}^H\mathbf{a}_{ik}\right|^2+\sigma_N^2}, \tag{17}$$

Algorithm 1 : Algorithm for transmit beamforming.

Initialization: Initialize $\mathbf{W}$ to a feasible value.

Repeat

Step 1: Update $\mathbf{y}$ by (15).

Step 2: Update $\boldsymbol{\beta}$ by solving $\mathcal{P}_{w_3}$ in (16).

Step 3: Update $\mathbf{W}$ by solving feasibility problem over $\mathbf{W}$ for fixed $\boldsymbol{\beta}$.

Until the value of the objective function converges.

where $\mathbf{a}_{ik} = \text{diag}\left(\mathbf{g}_k^H\right)\mathbf{H}\mathbf{w}_i$, $b_{ik} = \mathbf{f}_k^H\mathbf{w}_i$, and $\boldsymbol{\theta} = [\theta_{11}, \cdots, \theta_{1L}, \cdots, \theta_{NL}]^T$. Then the optimization problem $\mathcal{P}_\theta$, can be treated as a multiple ratio fractional programming problem [16]. Inspired by [15], we apply a quadratic transform to the objective function of $\mathcal{P}_\theta$ as

$$f(\boldsymbol{\theta},\boldsymbol{\lambda}) = \sum\nolimits_{k\in\mathcal{K}} \alpha_k \log_2\left(1+2\lambda_k\sqrt{P}\text{Re}\left\{b_{kk}+\boldsymbol{\theta}^H\mathbf{a}_{kk}\right\} - \lambda_k^2\left(P\sum\nolimits_{i\in\mathcal{K}'}\left|b_{ik}+\boldsymbol{\theta}^H\mathbf{a}_{ik}\right|^2+\sigma_N^2\right)\right), \tag{18}$$

where $\boldsymbol{\lambda} = [\lambda_1, \cdots, \lambda_K]^T$ are auxiliary variables introduced by the quadratic transformation. Thereby, we alternatively optimize $\boldsymbol{\theta}$ and $\boldsymbol{\lambda}$. For fixed $\boldsymbol{\theta}$, the optimal λ_k is found in closed-form as

$$\lambda_k^o = \frac{\sqrt{P}\text{Re}\left\{b_{kk}+\boldsymbol{\theta}^H\mathbf{a}_{kk}\right\}}{\ln(2)\left(P\sum_{i\in\mathcal{K}'}\left|b_{ik}+\boldsymbol{\theta}^H\mathbf{a}_{ik}\right|^2+\sigma_N^2\right)}. \tag{19}$$

***Remark* 1.** Without loss of generality, we confine that the matched outputs, for the beamforming vectors $(\mathbf{w}_k)$ and phase-shift vector $(\boldsymbol{\theta})$ with the channel responses produce, to a non-negative real desired signal term, i.e., $\left|b_{kk}+\boldsymbol{\theta}^H\mathbf{a}_{kk}\right| \approx \text{Re}(b_{kk}+\boldsymbol{\theta}^H\mathbf{a}_{kk})$. Our simulation results also reveals the validity of this approximation. This is because our algorithm maximizes in an iterative manner the weighted sum-rate by co-phasing the desired signal component while minimizing the inter-user interference.

Then, in the resulting optimization problem, we need to optimize $\boldsymbol{\theta}$ for given $\boldsymbol{\lambda}$. First, by expanding $\left|b_{ik}+\boldsymbol{\theta}^H\mathbf{a}_{ik}\right|^2$ and then applying a several mathematical manipulations, the objective function in (18) can be rewritten as

$$f(\boldsymbol{\theta}) = \sum\nolimits_{k\in\mathcal{K}} \alpha_k \log_2\left(1-\boldsymbol{\theta}^H\mathbf{U}_k\boldsymbol{\theta}+2\text{Re}\left\{\boldsymbol{\theta}^H\mathbf{v}_k\right\}+c_k\right), \tag{20}$$

where $\mathbf{U}_k$, $\mathbf{v}_k$, and c_k are defined as

$$\mathbf{U}_k = (\lambda_k^o)^2 P\sum\nolimits_{k\in\mathcal{K}'}\mathbf{a}_{ik}\mathbf{a}_{ik}^H, \tag{21}$$

$$\mathbf{v}_k = 2\lambda_k^o\sqrt{P}\mathbf{a}_{kk} - (\lambda_k^o)^2 P\sum\nolimits_{k\in\mathcal{K}'} b_{ik}^*\mathbf{a}_{ik}, \tag{22}$$

$$c_k = 2\lambda_k^o\sqrt{P}\text{Re}\{b_{kk}\} - (\lambda_k^o)^2\left(P\sum\nolimits_{k\in\mathcal{K}'}|b_{ik}|^2+\sigma_N^2\right). \tag{23}$$

Next, the corresponding optimization problem can be given as

$$\mathcal{P}_{\theta_1}: \underset{\boldsymbol{\theta}}{\text{maximize}} \; f(\boldsymbol{\theta}), \tag{24a}$$

$$\text{subject to } |\theta_{nl}| \leq 1, \forall n, l. \tag{24b}$$

Due to the fact that $\mathbf{a}_{ik}\mathbf{a}_{ik}^H$ is a positive-definite matrix for all i and k, $\mathbf{U}_k$ is a positive-definite matrix. Thus, the objective function, $f(\boldsymbol{\theta})$, is a quadratic concave function of $\boldsymbol{\theta}$. Consequently, $\mathcal{P}_{\theta_1}$ can be solved as a quadratically constrained quadratic program (QCQP). The algorithm for solving $\mathcal{P}_\theta$ is given in Algorithm 2.

Algorithm 2 : Algorithm for phase-shift optimization.

Initialization: Initialize $\boldsymbol{\theta}$ to a feasible value.
Repeat
Step 1: Update $\boldsymbol{\lambda}$ by (19).
Step 2: Update $\boldsymbol{\theta}$ by solving $\mathcal{P}_{\theta_1}$ in (24).
Until the value of the objective function converges.

***Remark* 2.** Algorithm 1 and Algorithm 2 summarize the proposed optimization techniques for solving $\mathbf{W}$ by fixing $\boldsymbol{\Theta}$ and for solving $\boldsymbol{\Theta}$ by fixing $\mathbf{W}$ once the original problem, $\mathcal{P}_1$, is decoupled into two sub-problems. $\mathcal{P}_1$ can then be solved iteratively using an alternating optimization technique. First, we quantify the SINR in (5) upon initializing $\mathbf{W}$ and $\boldsymbol{\Theta}$, and then better solutions for $\mathbf{W}$ and $\boldsymbol{\Theta}$ are updated in each iteration. This process continues until there is no further improvement, i.e., it is subjected to a stopping criterion such that the increment of the normalized objective function is less than $\epsilon = 10^{-4}$.

C. Computational Complexity

The proposed alternating optimization solution is a multi-stage iterative algorithm. Here, the outer loop has two sub-problems for optimizing $\mathbf{W}$ and $\boldsymbol{\Theta}$. Each sub-problem requires an iterative updating method to solve. Specifically, the computational complexities of Algorithm 1 and Algorithm 2 are centered in the step 3 and step 2, respectively. Moreover, CVX in Matlab uses SDPT3 solver for solving the proposed optimization problems. Thus, the computational complexities of the Algorithm 1 and Algorithm 2 are $\mathcal{O}(K^3)$ and $\mathcal{O}(N^3L^3)$, respectively [17], [18]. Hence, the total complexity of the proposed alternating optimization solution is $\mathcal{O}(I_o(I_wK^3 + I_\theta N^3L^3))$, where I_w, I_θ, and I_o are the iteration numbers of Algorithm 1, Algorithm 2, and the overall algorithm (outer loop), respectively.

IV. Numerical Results

In this Section, we evaluate the performance of the proposed system numerically. Our simulation parameters can be summarized as follows: $\zeta_{v_{ab}} = (d_0/d_{ab})^\nu \times 10^{\psi_{ab}/10}$, where $d_0 = 1$ m is the reference distance, d_{ab} is the transmission distance between node a and node b, and $\nu = 2.4$ is the path-loss exponent. Moreover, $10^{\psi/10}$ captures the shadow fading with $\psi_{ab} \sim \mathcal{N}(0, 8)$. The APs and RISs are uniformly distributed over an area of $800 \times 800\,\mathrm{m}^2$, while the users are randomly distributed. The AWGN variance, σ_N^2 is modeled as $\sigma_N^2 = 10\log_{10}(N_0 B N_f)$ dB, where $N_0 = -174$ dBm/Hz, $B = 20$ MHz is the bandwidth, and $N_f = 10$ dB is the noise figure. Moreover, all the users are assigned with equal priorities, i.e., $\alpha_i = 1/K, \forall i$.

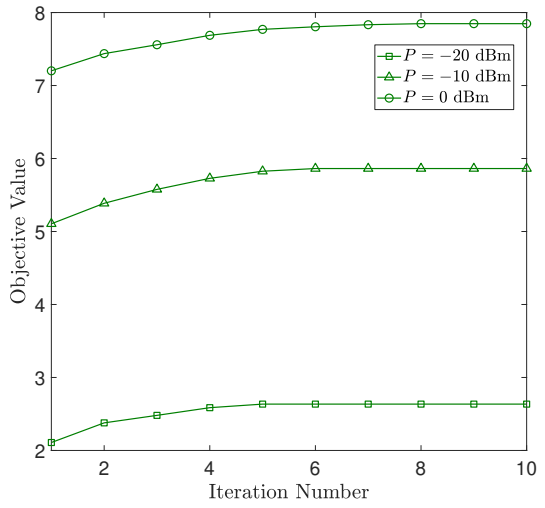

Fig. 2. The convergence of the objective value for $M = 16$, $N = 4$, $L = 32$, and $K = 2$.

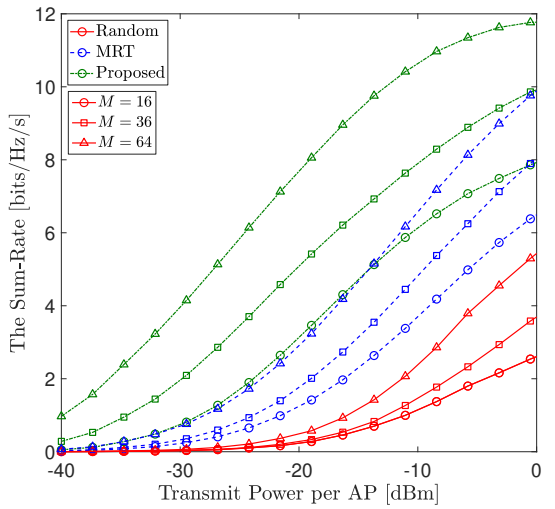

Fig. 3. The sum-rate for $M = \{16, 36, 64\}$, $N = 4$, $L = 32$, and $K = 2$.

In Fig. 2, we investigate the convergence behavior of the proposed algorithm for three different transmit power levels per AP. The objective function of the overall algorithm is the weighted sum-rate in (8a). The stopping condition for convergence is that the increment of the normalized objective function is less than $\epsilon = 10^{-4}$. As shown in Fig. 2, the weighted sum-rate obtained by combining Algorithms 1 and 2 increases rapidly and saturates as the number of outer loop iterations increases. Specifically, the proposed overall algorithm converges in less than 6 iterations regardless of the transmit power levels per AP.

In Fig. 3, we plot the system-wide average achievable sum-rate against the transmit power per AP by varying the number of APs as $M = \{16, 36, 64\}$. Three sets of sum-rate curves are plotted by adopting random beamforming, maximum ra-

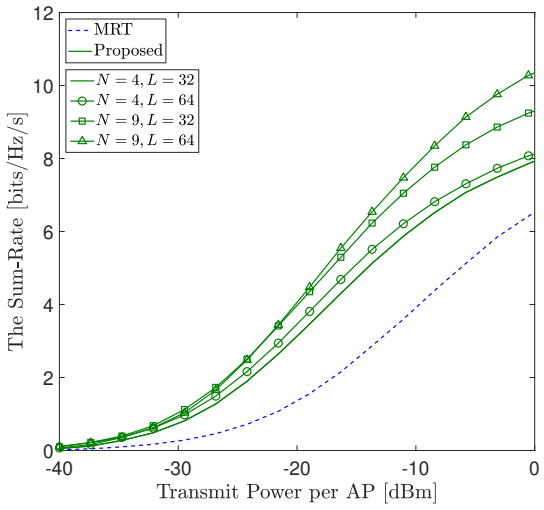

Fig. 4. The sum-rate for $M = 16$, $N = \{4, 9\}$, $L = \{32, 64\}$, and $K = 2$.

tio transmission (MRT) beamforming, and proposed optimal beamformers. In random beamforming, the precoders at the mth AP are designed by generating random $w_{mi}, \forall i$, such that $\sum_{i \in \mathcal{K}} |w_{mi}|^2 \leq 1$, whereas in MRT beamforming, it is assumed that the RISs are turned off and thereby adopting conjugate beamforming as in conventional cell-free mMIMO systems. Fig. 3 clearly depicts that higher the number of APs in the given geographical area, higher the achievable sum-rate regardless of the beamforming scheme. For instance, $M = 36$ and $M = 64$ cases provide sum-rate gains of 30.0% and 77.3%, respectively, compared to $M = 16$ case for the proposed optimal beamformers with -10 dBm of the transmit power per AP. Thus, it is observed that the deployment of distributed RISs within a cell-free mMIMO setup is beneficial in achieving a higher system-wide average sum-rate.

In Fig. 4, we study the effects of the numbers of RISs and reflecting elements. Thus, the achievable sum-rate is plotted as a function of the transmit power per AP for different combinations of $N = \{4, 9\}$ and $L = \{32, 64\}$. The achievable average sum-rate of the MRT beamforming with no RISs is also plotted for the purpose of comparisons. Fig. 4 reveals that when N or L increases, the achievable sum-rate can be improved. For example, the combinations of $\{N = 4, L = 64\}$, $\{N = 9, L = 32\}$, and $\{N = 9, L = 64\}$ provide sum-rate gains of 5.8%, 20.1%, and 27.4%, respectively, by the proposed techniques compared to the case of $\{N = 4, L = 32\}$ with -10 dBm transmit power per AP.

V. Conclusion

In this paper, a distributed RIS-assisted cell-free mMIMO setup has been investigated. Towards this end, a joint optimization problem for designing the transmit beamformers at the APs and passive phase-shift matrices at the RISs has been formulated to maximize the system-wide achievable weighted sum-rate under a transmit power constraint at the APs. An efficient alternating-optimization method has been employed to solve this joint optimization problem. The computation complexity and convergence behavior of this optimization solution have been investigated through our analysis and numerical results. It has been demonstrated that our proposed distributed RIS-assisted cell-free mMIMO setup achieves performance gains over the conventional counterpart in terms of the system-wide achievable average sum-rate. In addition, the overall algorithm requires fewer iterations to maximize the objective function, which implies that the proposed method has a high order of convergence. Thus, the proposed distributed RIS-assisted cell-free mMIMO system configuration may be beneficial in the development of next-generation wireless systems with significant spectral efficiency gains.

References

[1] A. Lozano, R. W. Heath, and J. G. Andrews, "Fundamental Limits of Cooperation," *IEEE Trans. Inf. Theory*, vol. 59, no. 9, pp. 5213–5226, 2013.

[2] H. Q. Ngo *et al.*, "Cell-Free Massive MIMO: Uniformly great service for everyone," in *IEEE 16th Int. Workshop on Signal Process. Adv. Wireless Commun. (SPAWC)*, 2015, pp. 201–205.

[3] ——, "Cell-Free Massive MIMO Versus Small Cells," *IEEE Trans. Wireless Commun.*, vol. 16, no. 3, pp. 1834–1850, Mar. 2017.

[4] C. Liaskos *et al.*, "A New Wireless Communication Paradigm Through Software-Controlled Metasurfaces," *IEEE Commun. Mag.*, vol. 56, no. 9, pp. 162–169, 2018.

[5] M. D. Renzo *et al.*, "Smart Radio Environments Empowered by Reconfigurable AI Meta-Surfaces: An idea whose time has come," *EURASIP J. Wireless Commun. Net.*, May 2019.

[6] D. L. Galappaththige, D. Kudathanthirige, and G. Amarasuriya, "Performance Analysis of Distributed Intelligent Reflective Surface Aided Communications," in *IEEE Global Commun. Conf.*, 2020, pp. 1–6.

[7] E. Basar *et al.*, "Wireless Communications Through Reconfigurable Intelligent Surfaces," *IEEE Access*, vol. 7, pp. 116 753–116 773, 2019.

[8] Q. Wu and R. Zhang, "Intelligent Reflecting Surface Enhanced Wireless Network via Joint Active and Passive Beamforming," *IEEE Trans. Wireless Commun.*, vol. 18, no. 11, pp. 5394–5409, 2019.

[9] D. L. Galappaththige, D. Kudathanthirige, and G. Amarasuriya, "Performance Analysis of IRS-Assisted Cell-Free Communication," in *IEEE Global Commun. Conf. (GLOBECOM)*, 2021, pp. 1–6.

[10] H. Hu *et al.*, "Multi-Intelligent Reflecting Surface Assisted Cell-free Massive MIMO Downlink Transmission," in *IEEE 21st Int. Conf. Commun. Technol. (ICCT)*, 2021, pp. 531–537.

[11] S. Huang *et al.*, "Decentralized Beamforming Design for Intelligent Reflecting Surface-Enhanced Cell-Free Networks," *IEEE Wireless Commun. Lett.*, vol. 10, no. 3, pp. 673–677, 2021.

[12] M. Bashar *et al.*, "On the Performance of Reconfigurable Intelligent Surface-Aided Cell-Free Massive MIMO Uplink," in *IEEE Global Commun. Conf.*, 2020, pp. 1–6.

[13] B. Al-Nahhas *et al.*, "RIS-Aided Cell-Free Massive MIMO: Performance Analysis and Competitiveness," in *IEEE Int. Conf. Commun. Workshops (ICC Workshops)*, 2021, pp. 1–6.

[14] Y. Zhang *et al.*, "Beyond Cell-Free MIMO: Energy Efficient Reconfigurable Intelligent Surface Aided Cell-Free MIMO Communications," *IEEE Trans. on Cogn. Commun. Netw.*, vol. 7, no. 2, pp. 412–426, 2021.

[15] K. Shen and W. Yu, "Fractional Programming for Communication Systems-Part I: Power Control and Beamforming," *IEEE Trans. Signal Process.*, vol. 66, no. 10, pp. 2616–2630, 2018.

[16] H. Guo *et al.*, "Weighted Sum-Rate Maximization for Intelligent Reflecting Surface Enhanced Wireless Networks," in *IEEE Global Commun. Conf. (GLOBECOM)*, 2019, pp. 1–6.

[17] A. Ben-Tal and A. S. Nemirovskiaei, *Lectures on Modern Convex Optimization: Analysis, Algorithms, and Engineering Applications*. USA: Society for Industrial and Applied Mathematics, 2001.

[18] J. S. Borrero, C. Gillen, and O. A. Prokopyev, "Fractional 0—1 Programming: Applications and Algorithms," *J. of Global Optimization*, vol. 69, no. 1, pp. 255–282, sep 2017.